Simulation of the electromagnetic vector field in the high-frequency components with dispersive materials

Bogusław Butryło[*]

Białystok Technical University
ul. Wiejska 45D, 15-351 Białystok, Poland

Abstract

This paper deals with parallel analysis of an electromagnetic problem for frequency-dependent materials. The solution of the linear wave equation is achieved using the finite element time domain method. A multi-pole Debye model approximates the memory of the dispersive material. The time-domain convolution is explicitly calculated using the integration by parts method. The linear recursive technique is implemented to estimate the convolution integral in each time step. The comparative study of two parallel implementations of the algorithm is presented. The discussed parallel versions are based on the domain decomposition paradigm and task decomposition scheme. The task decomposition is developed using some heuristic scheme of coupling of parallel tasks. The presented algorithms are executed over a distributed, homogeneous testbed. Some aspects connected with simulation of a broadband electromagnetic field in a dispersive and isotropic material are discussed.

1. Introduction

With the proliferation of wireless communication systems and digital high frequency electronic equipment, the need for efficient analysis of some complex material structures has emerged. Since the modern materials applied in

---

[*]*E-mail address:* butrylo@we.pb.edu.pl

the electronic and telecommunication technology are complex (e.g. composite materials, multi-layer materials, polymers), the resultant profile of electric permittivity is not trivial, and it should be taken into account in the numerical analysis [1]. Therefore, the computer-aided analysis of some broadband electromagnetic (EM) fields is of interest in modern technology and it is developed within computational electromagnetics (CEM) [2]. Numerical approximation of the wide-band EM phenomena can lead to a complex and large-scale numerical problem [3, 4]. The computational and memory costs of the CEM algorithm explicitly arise from restrictions of numerical integration of the constitutive, partial differential equations. The Nyquist's theory and the Courant-Friedrich-Levy (CFL) condition put the constraints on the mesh of the numerical model and the time step in the time integration scheme [5, 6]. Certainly, the specification of material data also determines properties of the algorithm.

This paper is focused on parallel formulation of the finite element (FE) algorithm implemented to a broadband analysis of electromagnetic phenomena in a dispersive media. The developed software is based on the direct numerical integration of time dependent wave equation with dispersity and damping. Two forms of the distributed algorithm are compared. The common form of the algorithm is based on the domain decomposition paradigm. The properties of this algorithm are modified by implementation of a task decomposition scheme. In this form the mutually dependent linear and dispersive parts of the numerical model are processed separately and interlaced in the time integration scheme. The coupling between these parts can shape the form of the algorithm. The elaborated algorithms are implemented on the cluster of workstations, using the MPI library.

2. Problem statement

The susceptibility of some materials applied in modern electronic technology depends on the frequency of the electromagnetic wave $\underline{\chi}(\omega) = \varepsilon_r(\omega) - 1 = \chi'(\omega) - i\chi''(\omega)$. Since the susceptibility of real condensed media cannot be expressed in a simple form, some empirical profiles of susceptibility are approximated $\chi(\omega) \propto \chi_r(\omega)$. Depending on the properties of dielectric media and the spectrum of propagated EM wave, the real broadband profile of susceptibility $\underline{\chi}_r$ is approximated using the multi-pole formula with some basic kernels $\underline{\chi}_d(\omega)$ shifted in the frequency domain [1, 7]

$$\underline{\chi}_r(\omega) = \sum_{d=1}^{N_D} \underline{\chi}_d(\omega),$$

where ω is the angular frequency of the EM wave, and d is the index of a pole (Fig. 1). In a common approach, the fundamental susceptibility kernels are either the first order functions (i.e. Debye, Rocard-Powles-Debye) or the second order Lorentz models [**7, 8**].
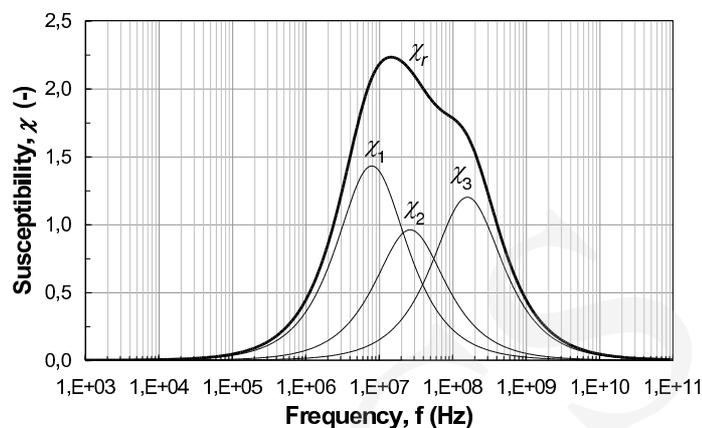

Fig. 1. Multi–pole approximation of the real susceptibility χ_r by the set of relaxation models

Assuming linear and isotropic properties of the analyzed model, the distribution of electromagnetic field **E** is expressed by the modified wave equation

$$\nabla^2 \boldsymbol{E} + \mu_0 \varepsilon_0 \frac{\partial^2}{\partial t^2} F^{-1} \left\{ \varepsilon_\infty + \chi_r(\omega) \right\} * \boldsymbol{E} + \mu_0 \sigma \frac{\partial \boldsymbol{E}}{\partial t} = 0,$$

with the multi–pole, time dependent susceptibility kernel within the convolution. After some rearrangements, the wave equation becomes the form

$$\nabla^2 \boldsymbol{E} + \mu_0 \varepsilon_0 \varepsilon_{r,\infty} \frac{\partial^2 \boldsymbol{E}}{\partial t^2} + \mu_0 \varepsilon_0 \sum_{d=1}^{N_D} \frac{\partial^2}{\partial t^2} \left(\chi_d(t) * \boldsymbol{E} \right) + \mu_0 \sigma \frac{\partial \boldsymbol{E}}{\partial t} = 0, \qquad (1)$$

where ε_0 is the permittivity of vacuum, ε_∞ is the optical permittivity (when the frequency of EM wave goes to some extremely-large values, near the optical spectrum), μ_0 is the permeability, and σ - the electric conductivity.

The convolution integral $\boldsymbol{c}_d(t) = \chi_d(t) * \boldsymbol{E}(t)$, $(d = 1, \ldots, N_D)$, in the presented formulation imposes the non-local operation into the common wave equation. The distribution of the electromagnetic field in any time step $\boldsymbol{E}(t) = \boldsymbol{E}(n\Delta t) = \boldsymbol{E}^n$ $(n = 0, 1, \ldots, N)$ is a direct solution of the modified equation (1). However, any convolution $\boldsymbol{c}(n\Delta t) = \boldsymbol{c}_d^n$ represents former evolution of the EM field $\boldsymbol{c}_d^n \succ \left\{ \boldsymbol{c}_d^{n-1}, \boldsymbol{E}^{n-1} \right\} \succ \left\{ \boldsymbol{c}_d^{n-2}, \boldsymbol{E}^{n-2} \right\} \succ \ldots \succ \left\{ \boldsymbol{c}_d^0, \boldsymbol{E}^0 \right\}$. Therefore, the set of convolution vectors $\{ \boldsymbol{c}_d \}$ $(d = 1, \ldots, N_D)$ represents the infinite memory of the dispersive material in the analyzed model.

$$E(\omega) = \sum_{h=1}^{N_h} E_h(\omega)$$

$$\chi(\omega) = \sum_{h=1}^{N_h} \chi_h(\omega)$$

Spectral decomposition

Domain (spatial) decomposition

Task decomposition

$$\Omega = \Omega_1 \cup \Omega_2 \cup \cdots \cup \Omega_D$$
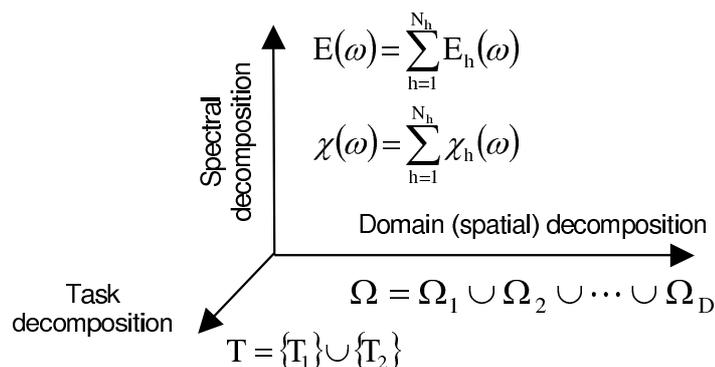
$$T = \{T_1\} \cup \{T_2\}$$

Fig. 2. Available methods of decomposition of a broadband, dispersive problem/algorithm

The dispersity of some material sub-structures makes the time domain algorithm hard in the parallel formulation. The memory cost, as well as self-dependent calculation of the electric field intensity $\boldsymbol{E}^n$ and the convolutions $\boldsymbol{c}_d^n$ are the main obstacles. The structure of the dispersive problem enables to implement (in the most sophisticated form) one of the three decomposition schemes, or any combination of these methods (Fig. 2). The spectral decomposition reduces the presented problem to the set of well known linear, narrow-band or single frequency models. In this case, the analysis of the broadband problem is replaced by some single-frequency sub-models, $\varepsilon_{r,n}(f_n) = const$. This formulation of the EM problem can be efficiently parallelized using both the frequency decomposition and the domain decomposition schemes. Any sub-model with initially calculated harmonic excitation of electromagnetic field and determined, frequency-independent material properties is calculated by a set of computing nodes. However, the ideal speedup of the FD algorithm does not coincide with the memory cost and accuracy of this approach. An inevitable error of approximation of the wide-band signal by the restricted set of harmonics degrades the results of computations. The calculated steady state distribution of electromagnetic field becomes deformed by a limited number of harmonics and Gibbs effects.

The spatial decomposition (DD) is well known and implemented in the computational electromagnetics [**5, 6, 9**]. Some prohibited constraints of that formulation (particularly, the memory cost), can be overcome by the supplementary task decomposition. Some large data structures connected with the dispersive part of the formulation can be moved to a complementary, separated set of computing nodes (PE_D).

3. Formulation of the finite element algorithm

Considering a three-dimensional, non-stationary electromagnetic problem in a bounded domain Ω, the weak form of the dispersive wave equation (1) takes the form [**2, 6, 9**]

$$
\int_{V_e} \boldsymbol{W}_j \varepsilon_0 \varepsilon_\infty \frac{\partial^2 e_i \boldsymbol{W}_i}{\partial t^2} dV + \int_{V_e} \boldsymbol{W}_j \varepsilon_0 \frac{\partial^2}{\partial t^2} \{\chi_r(t) * e_i \boldsymbol{W}_i\} dV + \int_{V_e} \boldsymbol{W}_j \sigma \frac{\partial e_i \boldsymbol{W}_i}{\partial t} dV
$$
$$
+ \int_{V_e} \frac{1}{\mu} (\triangle \times e_i \boldsymbol{W}_i)(\triangle \times \boldsymbol{W}_j) dV + \int_{S_{\infty,e}} \boldsymbol{W}_j \frac{1}{\mu c} \left(\frac{\partial e_i \boldsymbol{W}_i}{\partial t} \times \vec{\boldsymbol{n}} \right) dS = 0
$$

(2)

The geometry of the analyzed model is mapped by a structured tetrahedral mesh, $V_e \subset \Omega$. The $\boldsymbol{W}_i$ is the vector shape function for the i-th edge, since the set of degrees of freedom is spanned over the set of edges in the model. The time-dependent distribution of electromagnetic field is expressed by the vector of scalar values $\boldsymbol{E}^n = [e_i^n]^T$, $e_i^n \in \mathbb{R}$, $i = 1, \ldots, N_{DOF}$ [**2, 6**].

The convolution $\chi_r(t) * e_i(t)$ within the first integral approximates frequency-dependent properties of the material structures and it is calculated using the PLRC (Piecewise Linear Recursive Convolution) method [**7, 9**]. The wide-band profiles of susceptibility $\chi_r(\omega) = F\{\chi_r(t)\}$ of some materials are approximated by an experimental model based on the multi-pole Debye formula [**7, 8**]

$$
\chi_r(t) = F^{-1} \left\{ \sum_{d=1}^{N_D} \frac{\Delta \varepsilon_d}{1 + j\omega \tau_d} \right\} = \sum_{d=1}^{N_D} \frac{\Delta \varepsilon_d}{\tau_d} e^{-t/\tau_d} u(t),
$$

(3)

where $u(t)$ is the Haeviside's function, $\Delta \varepsilon_p$, τ_p are the decrement of the relative permittivity, and time of relaxation of the p-th pole, respectively.

Assembling equation (2) over all edges in the model results in the final large-scale matrix equation $\boldsymbol{A} \cdot \boldsymbol{E}^n = \boldsymbol{b}^n$, where $\boldsymbol{b}^n = f\left(\boldsymbol{E}^{n-1}, \boldsymbol{E}^{n-2}, \boldsymbol{c}^n\right)$. The final form of the time domain finite element algorithm for the dispersive problem consists of the step-by-step approximation of the convolution

$$
\forall_{d=1,\ldots,N_D} \quad \boldsymbol{c}_d^{n+1} = e^{-\Delta t/\tau_d} \boldsymbol{c}_d^n + \boldsymbol{E}^{n+1} \frac{\Delta \varepsilon_d \tau_d}{\Delta t} \left(\frac{\Delta t}{\tau_d} - 1 + e^{-\Delta t/\tau_d} \right)
$$
$$
+ \boldsymbol{E}^n \frac{\Delta \varepsilon_d \tau_d}{\Delta t} \left(1 - \frac{\Delta t}{\tau_d} e^{-\Delta t/\tau_d} - e^{-\Delta t/\tau_d} \right),
$$

$\dim(\boldsymbol{c}_d^n) = \dim(\boldsymbol{E}^n) = N_{DOF}$, and connected, step-by-step solution of the matrix equation derived from the Newmark-beta time integration scheme [**7, 8,**

9, 10]

$$(\boldsymbol{A}_L + \boldsymbol{A}_D) \cdot \boldsymbol{E}^{n+1} = (\boldsymbol{B}_L - \boldsymbol{B}_D) \cdot \boldsymbol{E}^n - \boldsymbol{C}_L \cdot \boldsymbol{E}^{n-1}$$
$$+ \sum_{d=1}^{N_D} \boldsymbol{F} \cdot \left(\left(2 - e^{-\Delta t/\tau_d} \right) \boldsymbol{c}_d^n - \boldsymbol{c}_d^{n-1} \right). \tag{4}$$

The entries of the $\boldsymbol{A}_L$, $\boldsymbol{B}_L$, $\boldsymbol{C}_L$ matrices (valid for frequency independent components of the formulation, $\varepsilon_\infty = const$) and the $\boldsymbol{A}_D$, $\boldsymbol{B}_D$, $\boldsymbol{F}$ matrices (connected with the dispersive part, $\chi_r(\omega) = var$) are

$$a_{L,ij} = \left(\varepsilon_0 \varepsilon_\infty + \frac{\Delta t \sigma}{2} \right) I_1 + \frac{\Delta t^2}{4\mu} I_2,$$

$$a_{D,ij} = \sum_{d=1}^{N_D} \varepsilon_0 \frac{\Delta \varepsilon_d \tau_d}{\Delta t} \left(\frac{\Delta t}{\tau_d} - 1 + e^{-\Delta t/\tau_d} \right) I_1,$$

$$b_{L,ij} = 2\varepsilon_0 \varepsilon_\infty I_1 - \frac{\Delta t^2}{2\mu} I_2,$$

$$b_{D,ij} = \sum_{d=1}^{N_D} \varepsilon_0 \frac{\Delta \varepsilon_d \tau_d}{\Delta t} \left(1 - \frac{\Delta t}{\tau_d} e^{-\Delta t/\tau_d} - e^{-\Delta t/\tau_d} \right) I_1$$

$$c_{L,ij} = \left(\varepsilon_0 \varepsilon_\infty - \frac{\Delta t \sigma}{2} \right) I_1 + \frac{\Delta t^2}{4\mu} I_2,$$

$$f_{ij} = \sum_{d=1}^{N_D} \varepsilon_0 I_1,$$

where the I_1 and I_2 integrals are the dot and cross products of basis functions, respectively

$$I_1 = \int_{V_e} \boldsymbol{W}_i \boldsymbol{W}_j dV,$$

$$I_2 = \int_{V_e} \left(\triangle \times \boldsymbol{W}_i \right) \left(\triangle \times \boldsymbol{W}_j \right) dV.$$

4. Parallel implementations of the FE algorithm

Due to the formulation presented above, two parallel implementations of the time domain algorithm are developed. They differ in the structure of tasks, and the method of coupling between the processing units.

The first approach is derived from the basic formulation of the parallel FE algorithm for some linear EM problems [**5, 6, 9**]. This version of the algorithm is developed using the domain decomposition (DD) paradigm. The number of computing units in the cluster (N_{PE}) and the size of analyzed model explicitly
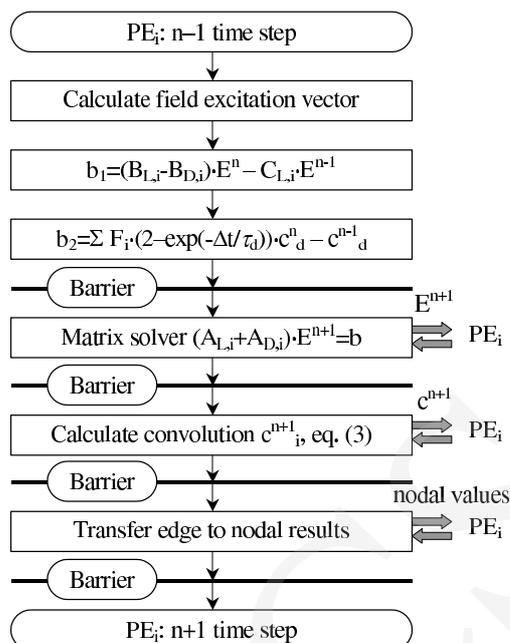
Fig. 3. Structure of tasks in the first version of the parallel algorithm

determine a stencil of sub-domains in the processing units. The FE mesh is decomposed into a number of sub-domains, and they are processed concurrently over different processing nodes. It results in the row-wise decomposition of the linear $\boldsymbol{A}_L$, $\boldsymbol{B}_L$, $\boldsymbol{C}_L$ and the dispersive $\boldsymbol{A}_D$, $\boldsymbol{B}_D$, $\boldsymbol{F}$ matrices. The non-overlapped sub-matrices $\boldsymbol{A}_{L,i}$, $\boldsymbol{B}_{L,i}$, $\boldsymbol{C}_{L,i}$, $\boldsymbol{A}_{D,i}$, $\boldsymbol{B}_{D,i}$, $\boldsymbol{F}_i$ are stored in the appropriate computing units P_{Ei} ($i = 1, \ldots, N_{PE}$). The geometrical binding of the sub-matrices creates the coherent representation of the FE model. The vectors of electric field intensity $\left\{\boldsymbol{E}^{n+1}, \boldsymbol{E}^n, \boldsymbol{E}^{n-1}\right\}$, the vectors of convolution $\left\{\boldsymbol{c}^{n+1}, \boldsymbol{c}^n\right\}$, and the data structures in the iterative matrix solver are duplicated in the processing units. The comprehensive forms of these vectors are obtained after $N_{PE} - 1$ broadcast commands in each time step.

According to the causality of the presented problem formulation, the computations of temporary value of the convolution vectors $\boldsymbol{c}_d^{n+1}$ are interlaced with iterative calculation of the time-dependent distribution of the electromagnetic field $\boldsymbol{E}^{n+1}$ (Fig. 3). The memory cost of the algorithm (Table 1) depends on the number of degrees of freedom (N_{DOF}), number of dispersive materials, and the order of dispersity (N_D). Therefore the total memory cost is reduced in the parallel version [**5, 6**].

Table 1.

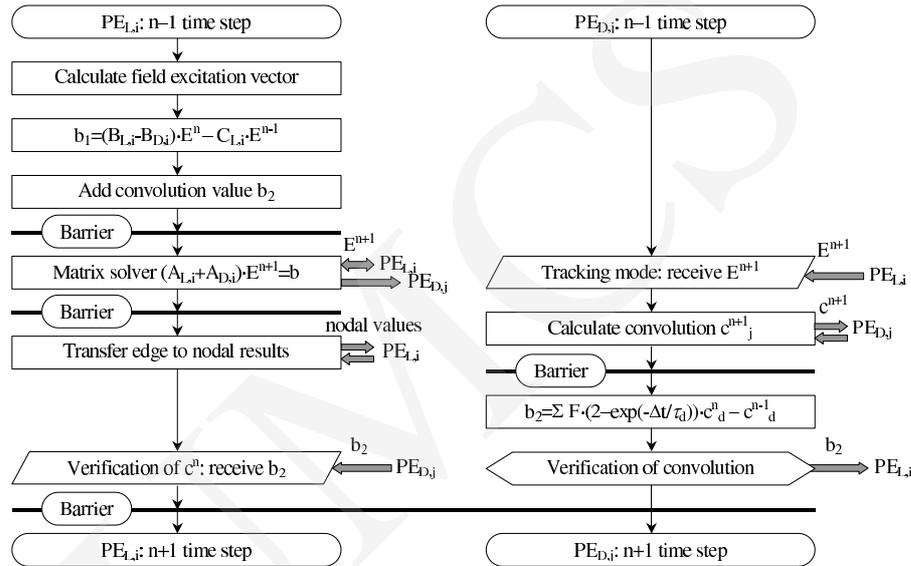| Symbol of the matrix or vector	Version 1 (domain decomposition)	Version 2 (domain and task decompositions)	
		Processing nodes	
	PE	PE_L	PE_D
$A_L + A_D$	DD: N_{DOF} / N_{PE}	DD: $N_{DOF} / N_{PE,L}$	-
$B_L + B_D$	DD: N_{DOF} / N_{PE}	DD: $N_{DOF} / N_{PE,L}$	-
C_L	DD: N_{DOF} / N_{PE}	DD: $N_{DOF} / N_{PE,L}$	-
F	DD: N_{DOF} / N_{PE}	-	DD: N_{DOF} / N_{PE}
E^n	N_{DOF}	N_{DOF}	N_{DOF}
E^{n-1}, E^{n-2}	N_{DOF}	N_{DOF}	-
c^n_d	$N_D \cdot N_{DOF}$	-	DD: $(N_D \cdot N_{DOF})/N_{PE,D}$

Fig. 4. Decomposition of computations among threads for a single time step

The second version of the algorithm is designed using the domain decomposition paradigm in conjunction with the task decomposition. This implementation works with two pre-defined sub-sets of the self-dependent jobs (Fig. 4). The distinguished two types of tasks are assigned to $PE_{L,i}$ $(i = 1, \ldots, N_{PE,l})$ or $PE_{D,j}$ $(j = 1, \ldots, N_{PE,d})$ computing nodes, respectively.

The extended, linear part of the formulation is processed by the $PE_{L,i}$ nodes. It consists of the data structures connected with the linear form of the model and an additive part of the dispersive formulation. The $\boldsymbol{A}_{D,i}$ and $\boldsymbol{B}_{D,i}$ sub-matrices are assembled with the $\boldsymbol{A}_{L,i}$ and $\boldsymbol{B}_{L,i}$ matrices respectively, and no additional memory in the computer system is needed. The communication pattern of this part is limited to the $PE_{L,i}$ nodes. The common work of the $PE_{L,i}$ nodes results

in the step-by-step calculation of the distribution of electromagnetic field $\boldsymbol{E}^{n+1}$. Since the geometry of the FE model is decomposed over the $N_{PE,L}$ computing nodes, the local results are exchanged and concatenated over this set of the nodes. The final calculated distribution of electromagnetic field in each time step is broadcast to both the $PE_{L,i}$ and the $PE_{D,j}$ computing units.

The $\boldsymbol{F}$ matrices and the set of sub-vectors of convolution $\left\{\boldsymbol{c}_d^{n+1}, \boldsymbol{c}_d^n\right\}$, related to the strictly dispersive part of the problem, are decomposed over the $N_{PE,d}$ nodes. These data structures are not allocated in the $PE_{L,i}$ nodes (Table 1). The stencil of the domain decomposition of the dispersive part differs from the linear part, since these sets of computing nodes are not equivalent in a general case. The $PE_{D,j}$ nodes work in a silent, monitoring mode. They collect the values of the electric field intensity $\boldsymbol{E}^{n+1}$ from the $PE_{L,i}$, and calculate the current state of the convolution vectors $\boldsymbol{c}_{n+1,p}$. These nodes monitor the last components of equation (4), related to the time-dependent vectors of the convolution $\left\{\boldsymbol{c}_d^{n+1}, \boldsymbol{c}_d^n\right\}$. When the modified value of the convolution vector $\boldsymbol{c}_d^{n+1}$ does not exceed a predefined threshold level, the convolution components in the first set of computing nodes $PE_{L,i}$ are approximated using the linear function. Otherwise, if the time-dependent, accumulated changes in the dispersive part of the problem cannot be neglected, the modified $\boldsymbol{b}_2$ vectors are transferred to $PE_{L,i}$ nodes (Fig. 4). In this way, the dispersive part of the matrix equation is refreshed. The approximate value of the convolution is injected to the $PE_{L,i}$ nodes. The distribution of electromagnetic field in the next time step is calculated with the refreshed value of convolution.

The relations between the $PE_{L,i}$ and $PE_{D,j}$ nodes are not symmetrical (Fig. 4). The data from $PE_{L,i}$ to $PE_{D,j}$ nodes are transferred at the end of each time step. This operation does not disturb the general structure and properties of the algorithm, since the $PE_{L,i}$ nodes must exchange the information about distribution of EM field in each time step. The $PE_{D,j}$ and $PE_{L,i}$ are linked only in some selected steps. Assuming the constant threshold level for the turning communication, the number of connections $PE_{D,j} \rightarrow PE_{L,i}$ depends on the size of dispersive structure in the model, the order of dispersity and the current, local value of derivative of the electromagnetic field $\boldsymbol{E}^{n+1}$, $\boldsymbol{E}^n$ in the model.

The coupling between the linear and dispersive sub-tasks is derived from a heuristic formula. The massive data transfers from the $PE_{D,j}$ to $PE_{L,i}$ nodes and refreshing of the convolution is triggered when the mean square error of the approximated value and the real value of the convolution is larger than the assumed (predefined) threshold level.

5. Performance of the algorithm and concluding remarks

The properties of the presented algorithms are determined using a benchmark problem, where the transient state is caused by the Gaussian electromagnetic pulse

$$\boldsymbol{E}_{inc}(x, y, z, t) = E_{\max} \exp\left(-\alpha^2 \left(t - \delta\right)^2\right) \vec{1}_z,$$

$$E_{\max} = 1 \text{ V/m}, \quad \alpha = 2 \cdot 10^{11} \text{s}^{-1}, \quad \delta = 4 \cdot 10^{-10} \text{s}.$$

This broadband pulse illuminates a linear cuboidal body with a dispersive layer. The dispersity of the body is approximated by the third order Debye model (3): $\Delta\varepsilon_1 = 2.4$ F/m, $\tau_1 = 1$ ns, $\Delta\varepsilon_2 = 2.96$ F/m, $\tau_2 = 20$ ns, $\Delta\varepsilon_3 = 1.9$ F/m, $\tau_3 = 6$ ns (Fig. 1). Some wave effects connected with the interaction between the wave and the solid body are shown in Fig. 5.

The comparative results of the benchmark problem have been obtained in a homogeneous cluster of 64 dual SMP nodes connected by the Infiniband network. Each of the nodes is equipped with a two-processor board with either 1GB or 2GB of RAM, and two Intel Xeon 3.2GHz processors with Intel EM64T Technology. In these experiments, each MPI process is mapped to one processor. Fig. 6 presents the experimental speedup and scaled-speedup for the benchmark problem. In this case, the number of nodes in the linear and the dispersive sub-sets are equal, $N_{PE,L} = N_{PE,D}$.
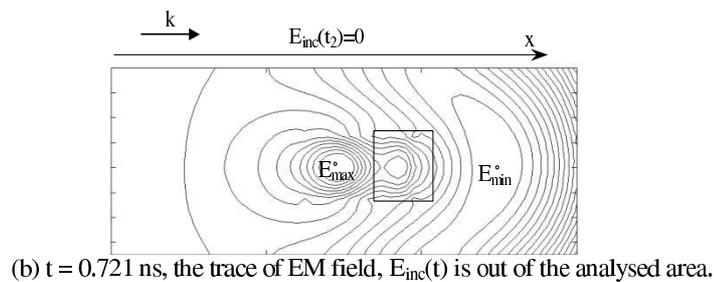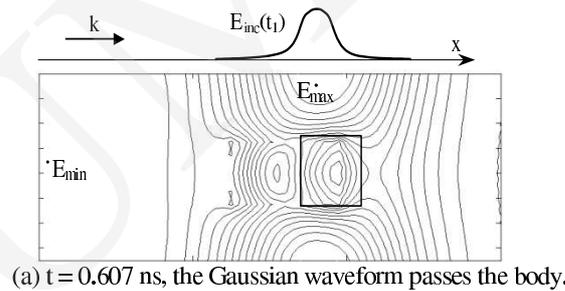

(a) t = 0.607 ns, the Gaussian waveform passes the body.

(b) t = 0.721 ns, the trace of EM field, $E_{inc}(t)$ is out of the analysed area.

Fig. 5. Some snapshots of the propagated electromagnetic wave $E_z(t)$ (the increment ΔE_z of the isolevels is 0.0625 V/m)
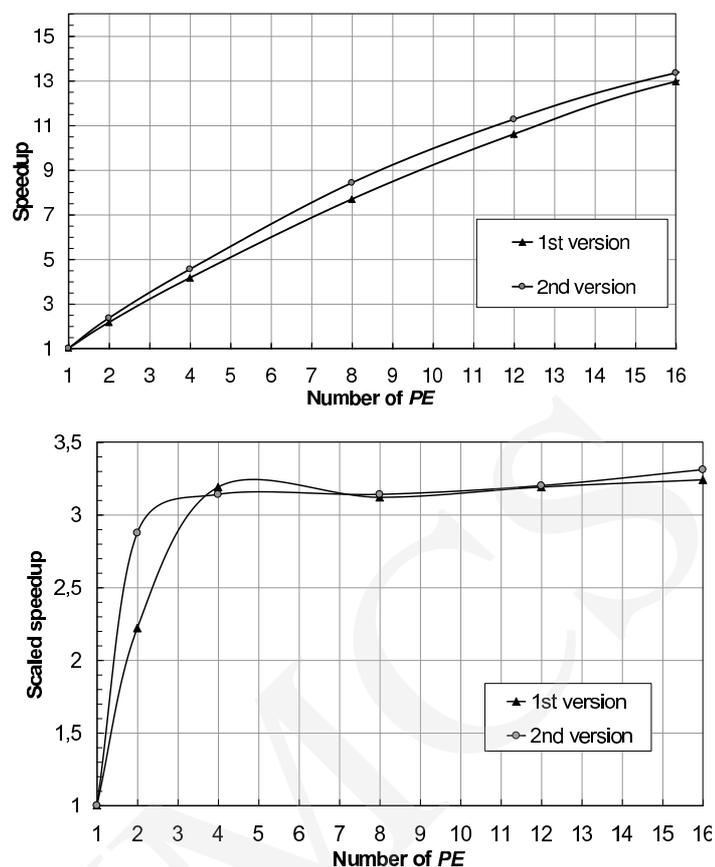
Fig. 6. Speedup and scaled speedup of the elaborated finite element algorithm

The main objective of the referred research is to develop a scalable, and flexible time domain algorithm for some dispersive EM problems. The wideband spectrum of the electromagnetic phenomena and physical properties of some materials introduce some extreme constraints for the time domain algorithms. The dispersity of material structures changes the structure and overall properties of the algorithm. A routine expansion of the linear formulation to frequency dependent materials can degrade the properties of the algorithm. Particularly, the memory cost increases, since it is proportional to the number of dispersive materials and the order of dispersity. The structure and performance of the time domain algorithm are shaped by the self-dependent, parallel computation of the electromagnetic field and the convolution.

Both presented implementations exploit displacement of the basic, structured matrices and duplication of the vectors of the state variables $\left\{\boldsymbol{E}^{n+1}, \boldsymbol{E}^{n}, \boldsymbol{E}^{n-1}\right\}$ and $\left\{\boldsymbol{c}^{n+1}, \boldsymbol{c}^{n}\right\}$. The introduction of the task decomposition enables to reduce

the elapsed time of computations. The communication pattern of the algorithm is not symmetrical. The performance of the second algorithm is improved by non-stable scheme of communication between the $PE_{L,i}$ and $PE_{D,j}$ nodes, based on the heuristic method. In this way the coupling between the processes can be matched to the form of the dispersity in the model, and the spectrum of the propagated field (i.e. the dynamics of the electromagnetic field). The quality of dispersity of the model as well as influence of the dispersive part of the formulation to the linear part of the formulation are partially validated. This form of the algorithm seems to be particularly useful in large-scale systems, when the data transfers increase as a result of a rising number of sub-domains in the FE parallel algorithm.

References

[1] Rao S. M. (ed.), *Time domain electromagnetics*, Academic Press, 1999.

[2] Lee J. F., Lee R., Cangellaris A., *Time-Domain Finite-Element Methods*, IEEE Transactions on Antennas and Propagation, IEEE Press 45(3) (1997) 430.

[3] Vollaire C., Nicolas L., Nicolas A., *Parallel computing for the finite element method*, The European Physical Journal Applied Physics 1 (1998) 305.

[4] Buyya R., *High Performance Cluster Computing*, vol. 2, Prentice Hall PTR, New Jersey, USA (1999).

[5] Butryło B., Musy F., Nicolas L., Parrussel R., Scorretti R., Vollaire C., *A survey of parallel solvers for the finite element method in computational electromagnetics*, Compel, Emerald Publishing 23(2) (2004) 531.

[6] Butryło B., Vollaire C., Nicolas L., *Limits of the Distributed Finite Element Time Domain Algorithm in Multi-computer Environment*, International Conference on Parallel Computing in Electrical Engineering: Parelec, Dresden, Germany, IEEE, Computer Society (2004) 194.

[7] Maradei F., *A frequency-dependent WETD formulation for dispersive materials*, IEEE Transactions on Magnetics, IEEE 37(5) (2001) 3303.

[8] Edelvik F., Strand B., *Frequency dispersive materials for 3-D hybrid solvers in time domain*, IEEE Transactions on Antennas and Propagation, IEEE 51(6) (2003) 1199.

[9] Butryło B., *Parallel Broadband Finite Element Time Domain Algorithm Implemented to Dispersive Electromagnetic Problem*, Lecture Notes in Computer Science, V. Malyshkin (Ed.): PaCT 2007, Springer-Verlag, LNCS 4671 (2007) 119.

[10] Navsariwala U., Gedney S., *An Unconditionally Stable Parallel Finite Element Time Domain Algorithm*, IEEE APS/URSI Symposium (1996).